

Updating 8 m 2MPZ and Independence Models

Quarterly Report for January 1 – March 31, 2013

by Brent Sherman

Supported by the Texas Carbon Management Program

and Carbon Capture Simulation Initiative

McKetta Department of Chemical Engineering

The University of Texas at Austin

April 30, 2013

Abstract

In addition to the continued work on the 2MPZ kinetic model, a new effort to expand the PZ model to include ions was begun this quarter. The 2MPZ kinetic model can match the experimental flux at low temperature, but due to improper centering of reaction constants the error builds moving away from 40 °C. In order to hasten calculations, the boundary layer was rediscritized to use fewer points without sacrificing accuracy. The number of points was reduced from fifty to thirty-two, which is only five more than that used for PZ. The expansion of the PZ model, dubbed the Ionic Model, involves no regression. The following ions were added from the Aspen Plus[®] databank: K⁺, Na⁺, NO₃⁻, SO₄²⁻, HCO₂⁻, and CH₃CO₂⁻. Their binary interaction parameters were set to default values, and then the solvent was simulated with greater ionic strength (salt effect) and additional alkalinity (alkalinity effect). It was found that practically speaking, both effects reduced the baseline capacity by ~20% from 0.8 mol CO₂/kg CO₂ free solvent. Future work will be to finish the 2MPZ kinetic model and begin viscosity sensitivity studies using a heat exchanger model.

Introduction

The overarching goal of this project is to develop a generic amine model and to use this model to systematically investigate the impact of amine properties on process performance. Subordinate goals include developing more models, developing new modeling methods, and ensuring consistency across models.

A generic amine model would allow for more rapid amine solvent screening. There are currently models for sundry piperazine (PZ) blends, including PZ with methyl diethanolamine (MDEA), 2-methylpiperazine (2MPZ), 2-amino-2-methyl-1-propanol (AMP), and aminoethylpiperazine (AEP). All of these blends broaden the solid solubility window of PZ while minimally compromising its beneficial properties. Each of these models represents a substantial investment of man hours, and a streamlined process would speed up screening.

Immediate work focused on kinetic modeling of 8 m 2MPZ and updating the Independence model to include cations and anions. A kinetic model work enables process modeling of 8 m 2MPZ, while including ions in Independence simulates thermal degradation conditions. Additionally, by varying the ionic strength of the solvent, salt and alkalinity effects on system performance can be investigated.

Modeling Methods

Ionic Model

The Ionic Model (IM) is a modification of the Independence model (Frailie et al., 2013) to include the following cations and anions: K^+ , Na^+ , NO_3^- , SO_4^{2-} , HCO_2^- , and $CH_3CO_2^-$. These species were added from the Aspen Plus[®] component databank. As there are no experimental data readily available for regression, the e-NRTL interaction parameters were left at their default values. Equation 1 shows the form of an interaction parameter, where i is the molecule and j the ion-pair.

$$\tau_{i,j} = C_{i,j} + \frac{D_{i,j}}{T} + E_{i,j} \left[\frac{T_{ref} - T}{T} + \ln \left(\frac{T}{T_{ref}} \right) \right] \quad (1)$$

There are two sets of default values depending on whether i is an electrolyte or water. For an electrolyte or non-water species, $C_{i,j}$ is 10 while $C_{j,i}$ is -2 where i is the molecule and j is the electrolyte pair. For water and zwitterions, $C_{i,j}$ is 8 while $C_{j,i}$ is -4 where i is the zwitterion or water and j is the electrolyte pair. These defaults come from the Aspen Plus[®] software documentation.

In order to ensure charge balance, every ion is added with a counterion. Potassium was used to counterbalance all anions, with potassium itself added as $KHCO_3$, to take advantage of the equilibrium bicarbonate reaction already present in the model.

The concept of loading becomes more complex when working with ions, as cations contribute to alkalinity while anions detract in accordance with their equivalence. Nevertheless, the standard loading definition of moles of CO_2 per mole of alkalinity still applies.

8 m 2MPZ Kinetic Modeling

Having verified the thermodynamic model last quarter, this quarter the kinetic model was developed. This was done using a wetted wall column (WWC) Aspen Plus[®] simulation to adjust reaction rate constants, activation energies, and diffusion parameters to match experimental flux values within 20% (Plaza, 2011; Rochelle et al., 2012). The process flow diagram is shown in Figure 1.

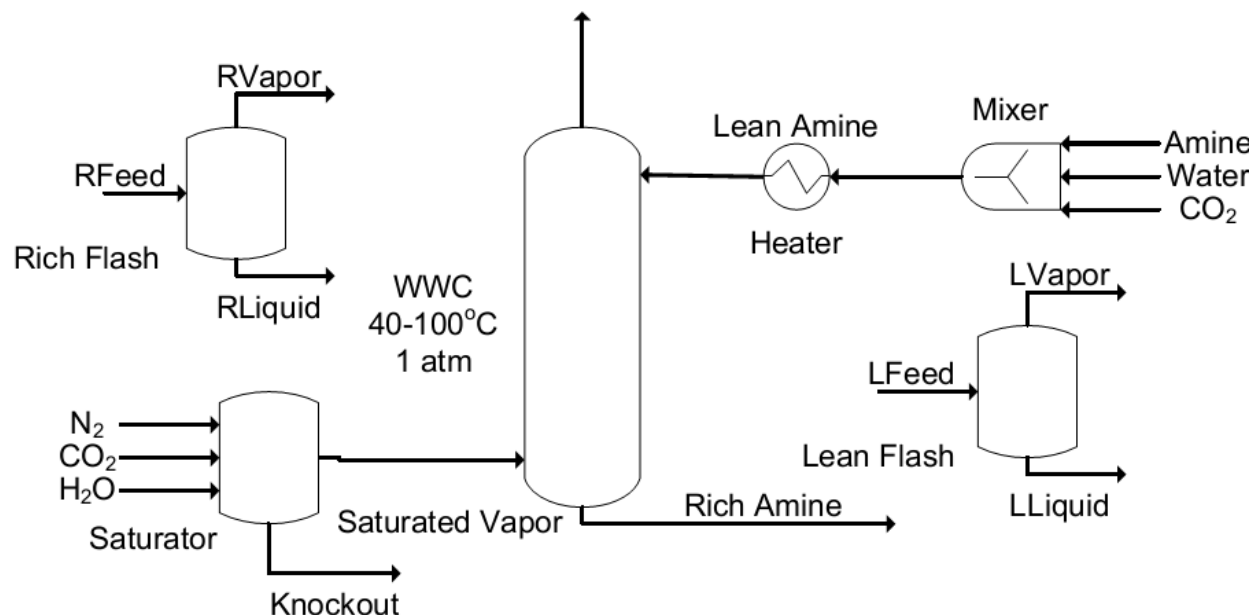


Figure 1: WWC process flow diagram for Aspen Plus[®]. This is similar to prior models.

The solvent is fed as three separate streams of amine, water, and CO₂. When mixed, the solvent heats up due to heat of mixing and speciation, and so a heater is used to return it to the desired temperature for isothermal operation. The entire WWC is operated isothermally to mimic laboratory conditions. The gas is fed to a flash vessel which saturates it with water. The gas and solvent are contacted in the WWC, which has the same height as the real life apparatus (9.1 cm) but a diameter that is 100x larger (0.44 cm x100). The rich and lean flash vessels flash the rich and lean amine streams, after the heater to calculate the equilibrium partial pressure of CO₂.

The complete reaction set used is shown in Table 1. The forward and reverse kinetic reactions are represented separately in Aspen Plus[®]. The forward reaction rates are calculated, and then the reverse rates are backcalculated using the reaction equilibrium constant. Using this setup, only one parameter at a time may be varied. The bicarbonate-forming reaction was fixed using values from literature (Ko & Li, 2000), while the dicarbamate-forming reaction was ratioed to the carbamate-forming reaction by assuming the Brønsted plot of PZ holds. This plot is shown in Figure 2. Thus, only the carbamate-forming reaction was regressed.

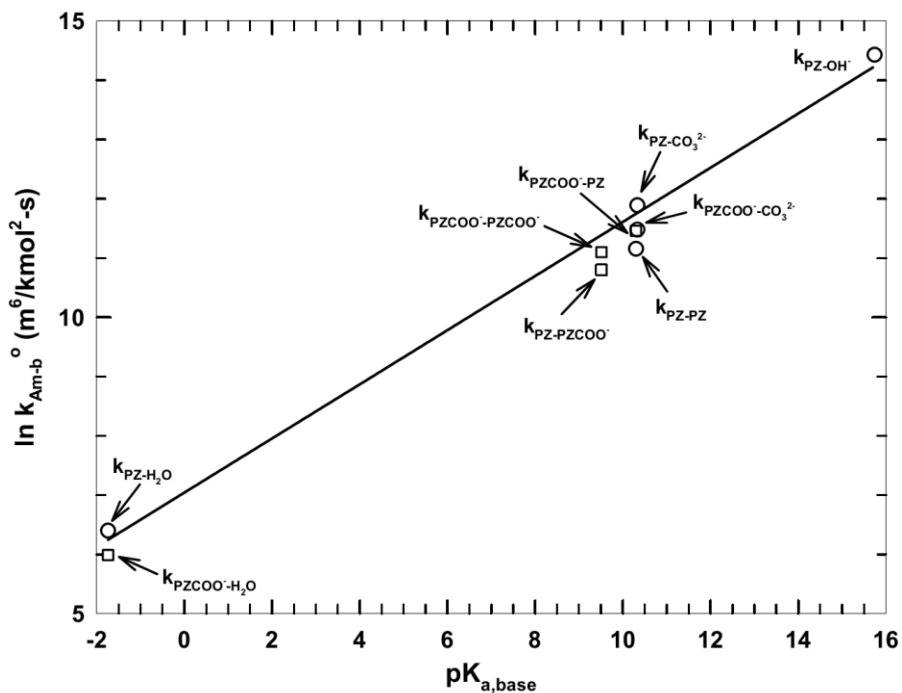


Figure 2: Brønsted plot showing the reaction rate constant (k_{Am-b}) vs the pK_a of a base for an amine catalyzed by a base, $k_{Am-base}$.

Table 1: Kinetic and equilibrium reactions used for 2MPZ. The equations at right show how the reaction rate constants are calculated.

<i>Reaction</i>	<i>Type</i>
$2\text{MPZCOO}^- + \text{H}_2\text{O} + \text{CO}_2 \leftrightarrow \text{H}_2\text{MPZCOO} + \text{HCO}_3^-$	Kinetic
$2\text{MPZ} + \text{CO}_2 \leftrightarrow 2\text{MPZH}^+ + 2\text{MPZCOO}^-$	
$2\text{MPZCOO}^- + \text{CO}_2 \leftrightarrow \text{H}_2\text{MPZCOO}^- + 2\text{MPZ}(\text{COO})_2^{2-}$	
	$K_{EQ} = \frac{k_f}{k_r}$
	$r_f = -k_f a_{Am} a_{\text{CO}_2} a_B$
	$r_r = k_r a_{Am\text{COO}^-} a_{\text{BH}^+}$
$2\text{MPZCOO}^- + 2\text{MPZH}^+ \leftrightarrow \text{H}_2\text{MPZCOO}^- + 2\text{MPZ}$	Equilibrium
$2\text{MPZ} + \text{HCO}_3^- \leftrightarrow 2\text{MPZH}^+ + \text{CO}_3^{2-}$	
	$-\ln K_j = \frac{\Delta G_j^\circ}{RT}$

Before regressing reaction rate constants, the experimental loading must be adjusted for errors in its measurement as well as any errors in the equilibrium model. This was previously done by matching the experimentally measured equilibrium partial pressure of CO_2 by adjusting the loading, but this proved inexact. Instead, the loading was adjusted until the strongest absorption and desorption points for one set of temperature and loading data could be met with less than 10% variation in the reaction constant. The loading is only adjusted up to 10% of the operational loading range, which for 2MPZ is 0.01 mol $\text{CO}_2/\text{mol alk}$.

Once this is completed for the extreme absorption and desorption points, the resulting reaction rate constants are used to make an Arrhenius plot of $\ln(k)$ vs $1/T$, whose slope is $R \cdot E_A$. Using a linear fit, the reaction pre-exponential can be found at any temperature. As the reactions are most important in the absorber, the pre-exponential value at 40 °C is used.

Results and Discussion

Ionic Model

As noted above, the Ionic Model is a modification of Independence to include ions of relevant species. This model was run at a concentration of 5 molal PZ with an eye towards natural gas capture applications. The two effects that can be explored through varying the concentration and type of ions added are 1) the salt effect, and 2) the alkalinity effect.

Practically speaking, both effects reduce the capacity and change the operational loading range – defined as the lean and rich loadings correspond to $P_{\text{CO}_2}^* = 0.5$ and 1.5 kPa – as summarized in Table 2.

Table 2: Amine properties. ΔH_{abs} at $P_{\text{CO}_2}^* = 1.5 \text{ kPa}$. Loading is defined in Equation 2.

Property	5 m PZ	5 m PZ + 1.05 m KNO ₃	5 m PZ + 1.05 m KHCO ₃
Loading range	0.39-0.31	0.37-0.32	0.40-0.34
$-\Delta H_{\text{abs}}$ (kJ/mol)	-70	-70	-70
ΔC (mol/kg CO ₂ free solvent)	0.80	0.61	0.66

Salt Effect

By increasing the ionic strength of the solvent through adding more ions (e.g., $^+ \text{NaNO}_3^-$) the overall polarity of the solvent will increase. The increasingly polar environment will stabilize the charged electrolytic species rather than neutral molecules. This effect is coupled with the change in the dominant reaction across the operational loading range. At low CO₂ loading, $2 \text{ PZ} + \text{CO}_2 \leftrightarrow \text{PZH}^+ + \text{PZCOO}^-$ dominates while at higher loading, $\text{PZH}^+ + \text{PZCOO}^- + \text{CO}_2 \leftrightarrow 2 \text{ }^+ \text{HPZCOO}^-$ dominates. This can be seen from the stoichiometry plot of Figure 3. Comparing these two reactions in light of the increasing stabilization of electrolytes with increased ionic strength, the former reaction will be pushed to the right while the latter will be pushed to the left. (As the zwitterion has a net-neutral charge, it behaves more as a molecule than as an electrolyte.) This effect is visible in the VLE curves of Figure 4. The change in VLE negligibly impacts the heat of absorption in the operational loading range as depicted in Figure 5. The increased stability of electrolytes is reflected in the speciation of Figure 6 primarily by the more rapid depletion of free PZ in favor of electrolytes. Similar results were previously found for potassium carbonate enhanced with PZ (Cullinane, 2005).

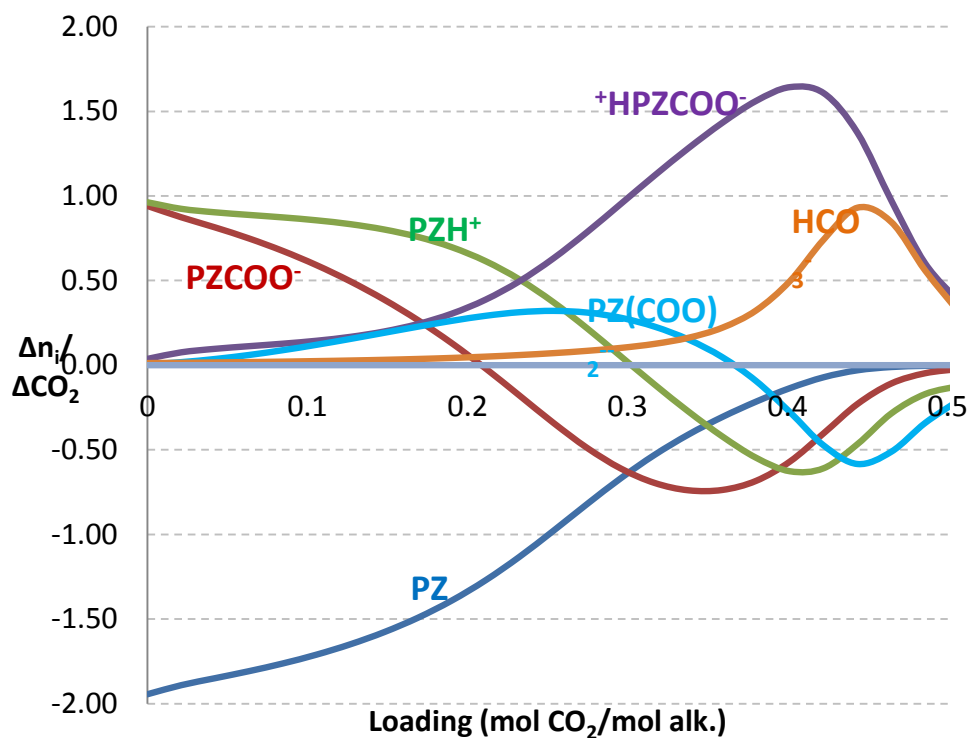


Figure 3: 5 m PZ stoichiometry at 40 °C showing the chemistry switch at around 0.25 mol CO₂/mol alk.

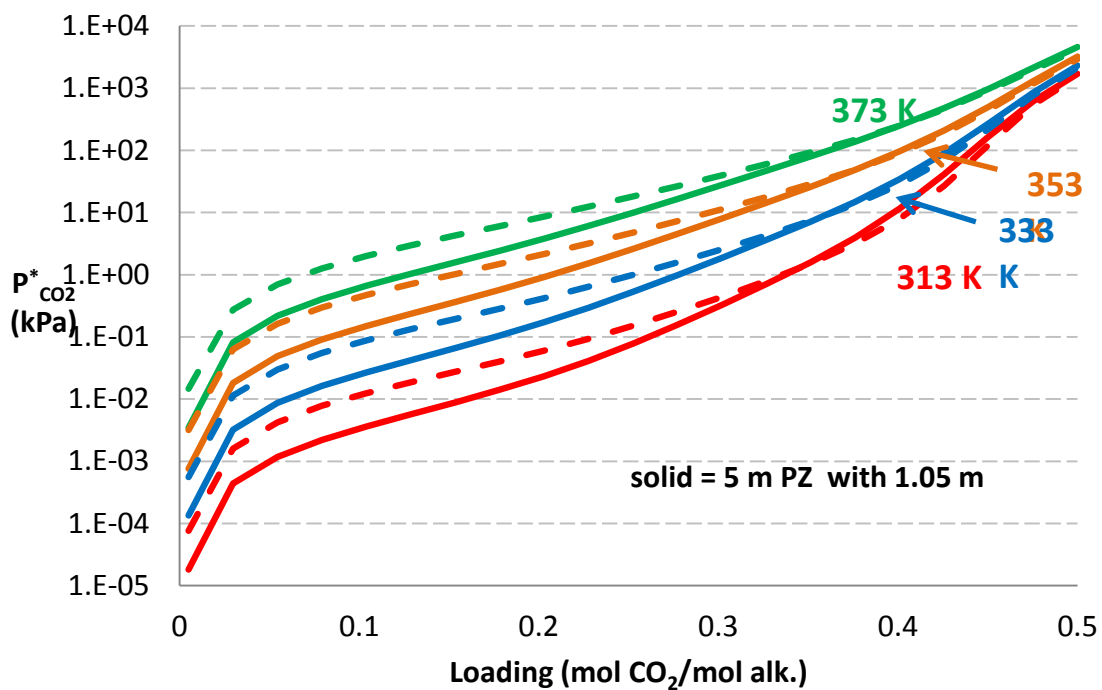


Figure 4: VLE of 5 m PZ (dashed) and 5 m PZ with 1.05 m NaNO₃ (solid).

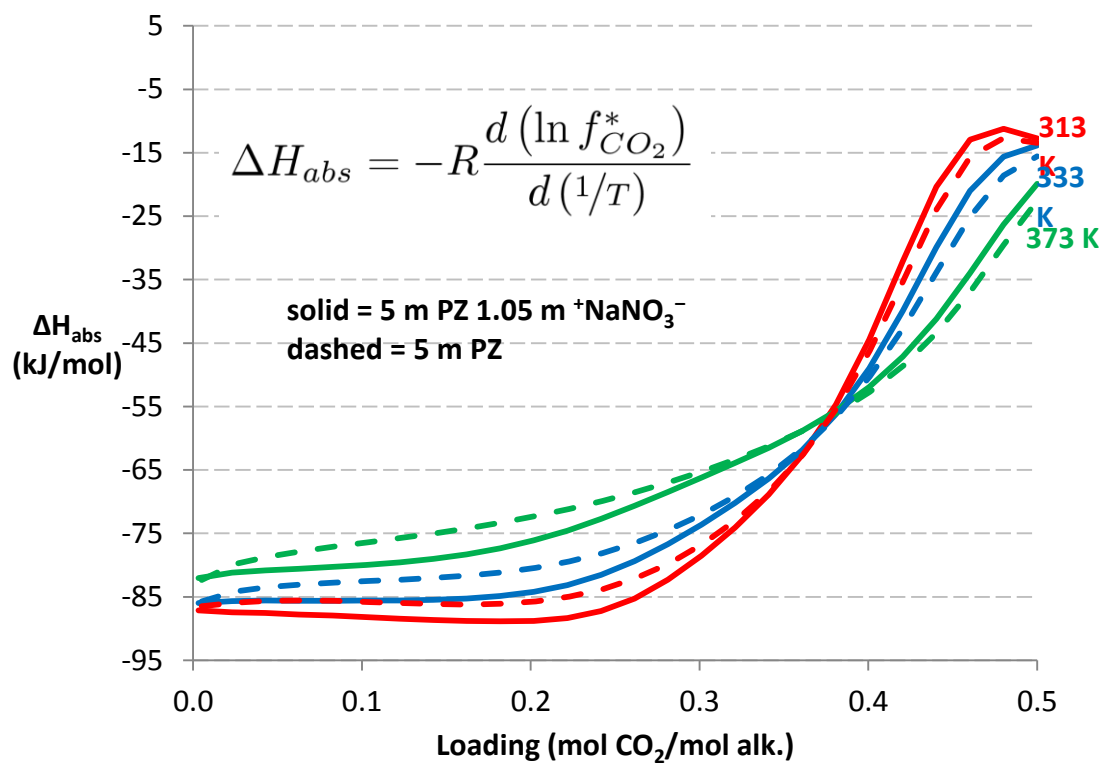


Figure 5: Heat of absorption comparison. ΔH_{abs} is lower, but not in the operational range.

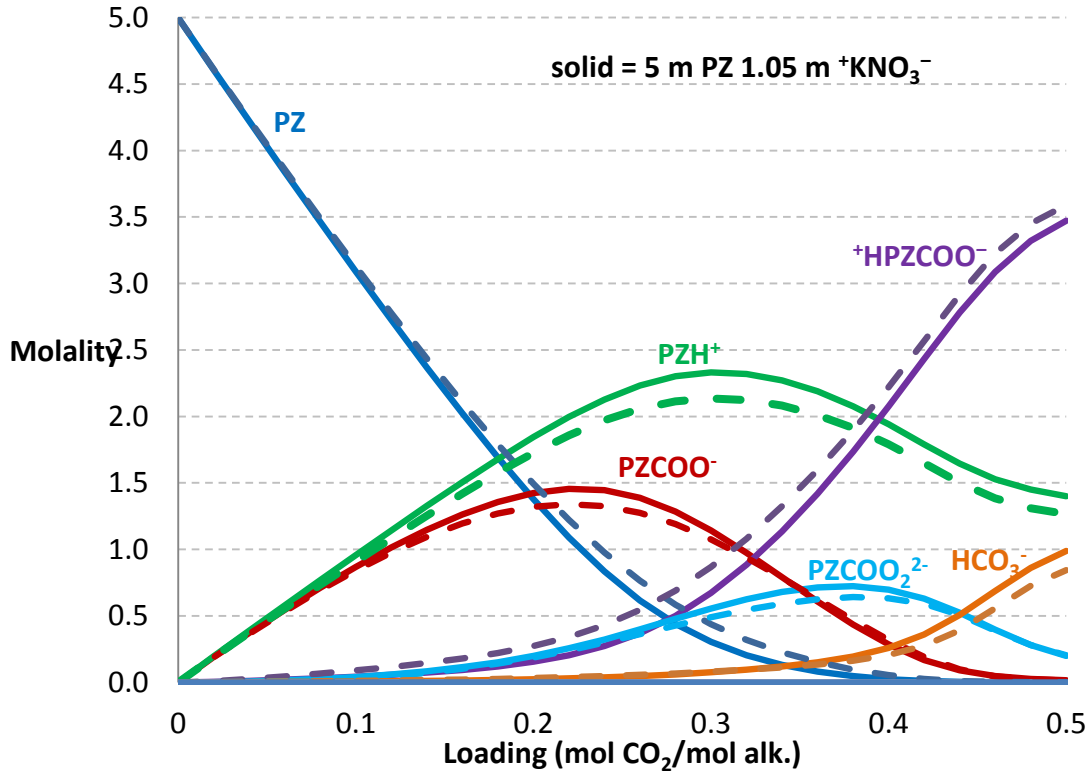


Figure 6: Predicted speciation at 40 °C. Increased ionic strength leads to quicker depletion of free PZ.

Alkalinity Effect

The alkalinity effect is similar to the salt effect in that the ionic strength of the system is also increased. However, whereas before a CO_2 -free anion was used, now potassium is added as KHCO_3^- , which increases the overall alkalinity of the system. This means that the loading is now calculated as,

$$\alpha = \frac{\text{mol } \text{CO}_2 + \text{mol } \text{HCO}_3^-}{2 * \text{mol } \text{PZ} + \text{mol } \text{K}^+} \quad (2)$$

For this reason, all of the following graphs will not start at zero loading. As with the salt effect, the additional ionic strength stabilizes electrolytes and now the increased alkalinity shifts the loadings to the richer end. This can be seen in the VLE, the heat of absorption, and the speciation, which are Figures 7, 8, and 9, respectively.

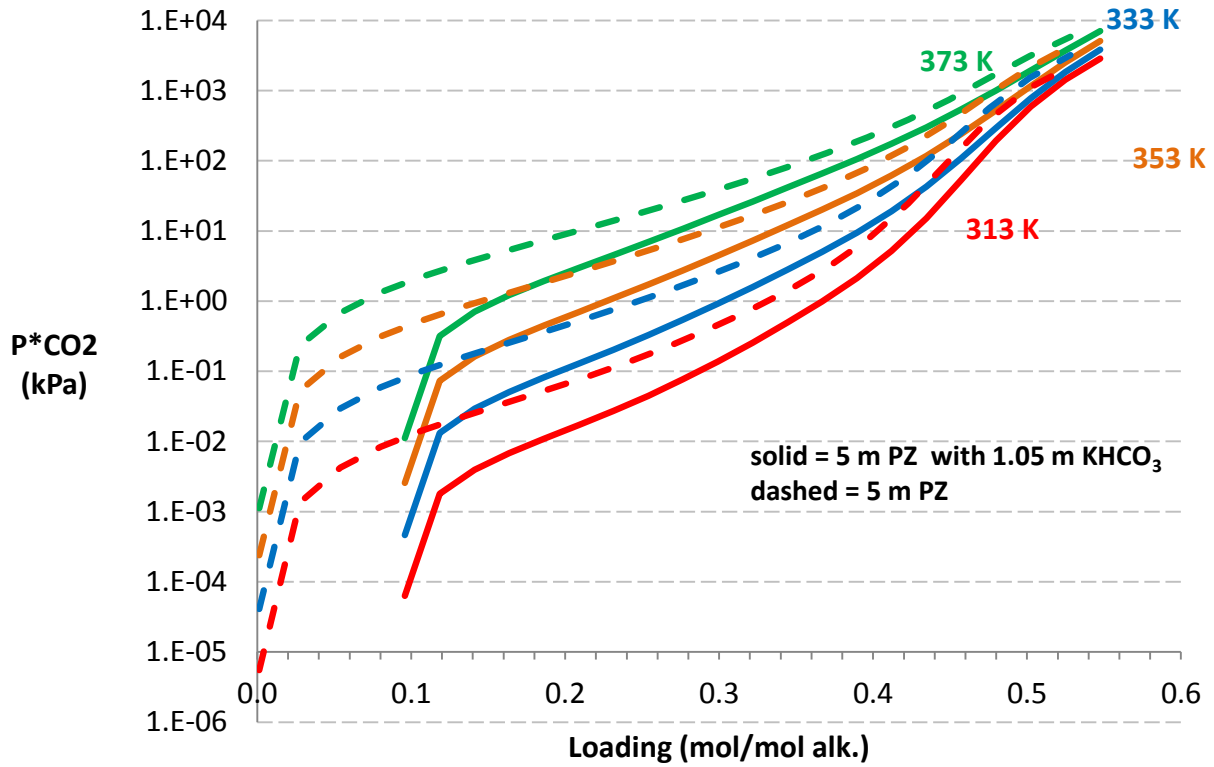


Figure 7: Effect of adding alkalinity as KHCO_3 on CO_2 solubility in 5 m PZ

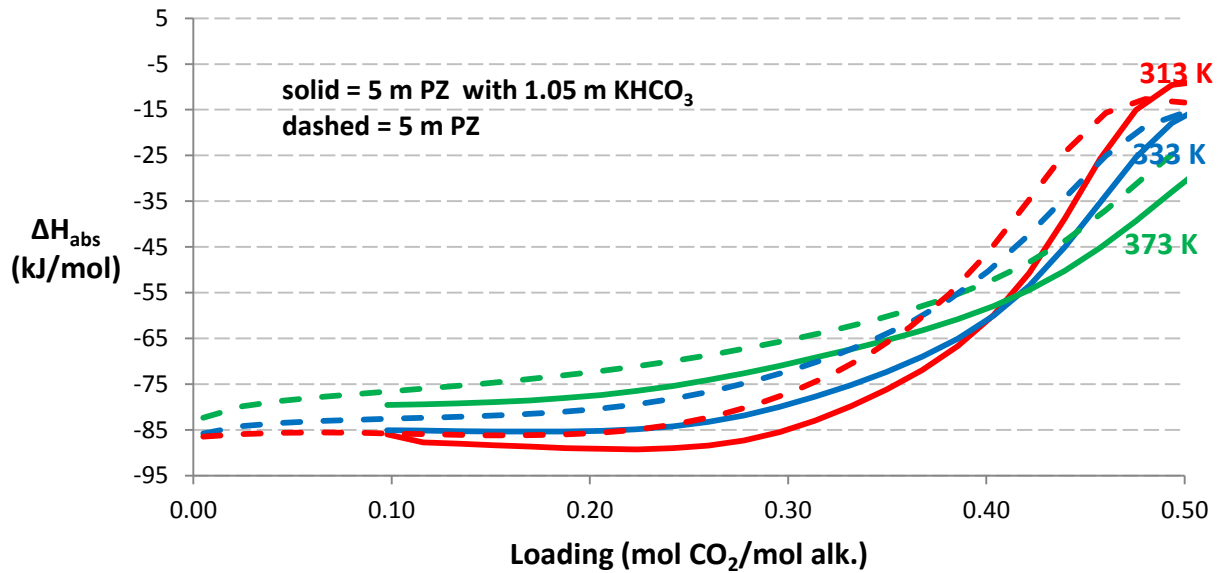


Figure 8: Effect of KHCO_3 alkalinity on heat of CO_2 absorption in 5 m PZ.

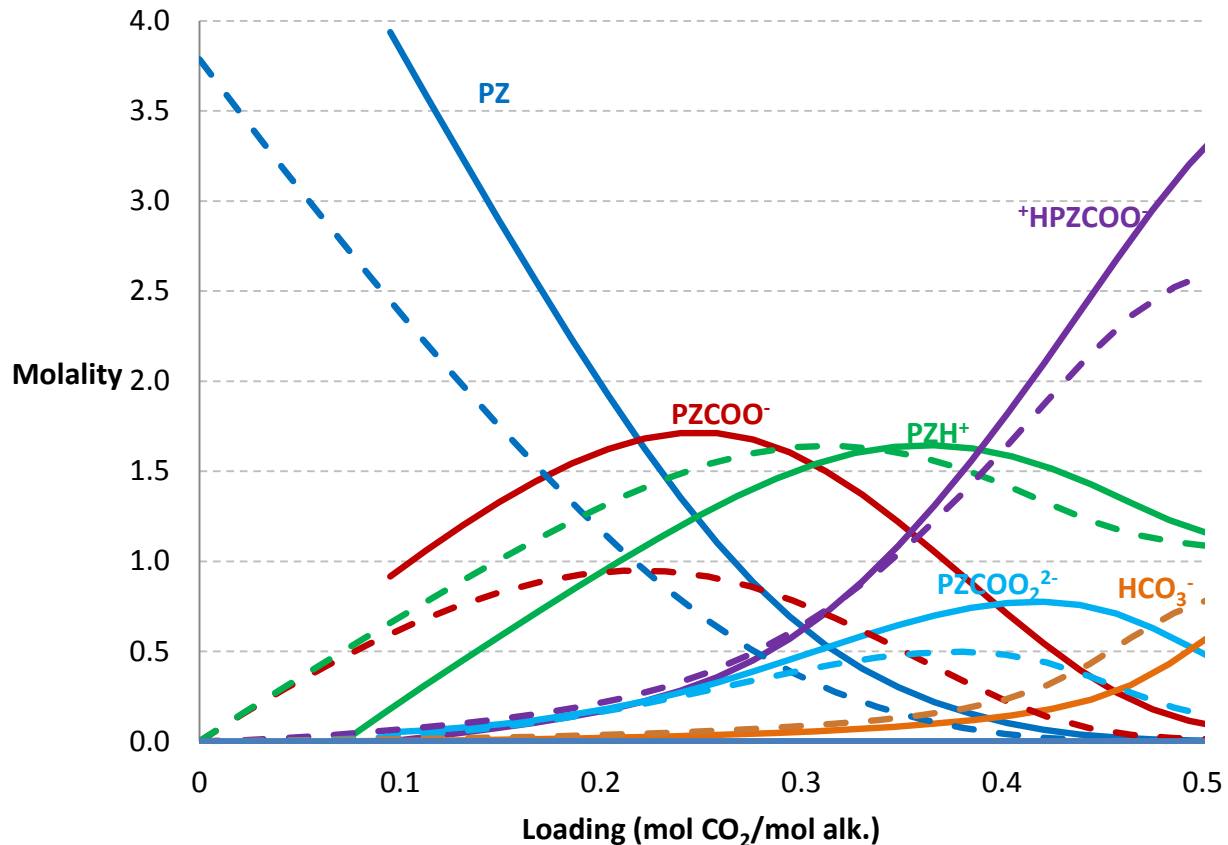


Figure 9: Predicted speciation at 40 °C. solid lines: 5 m PZ with 1.05 m KHCO₃, dashed lines: 5 m PZ. Everything has shifted to a higher loading.

8 m 2MPZ Kinetic Modeling

The experimental reaction flux has not yet been matched in Aspen Plus[®] as can be seen in Figures 10 and 11. The 40 °C data are well matched, but due to improperly centering the reaction set, the error grows more pronounced as the temperature increases. This problem has been identified, and the solution will be implemented shortly.

Aspen Plus[®] discretizes the boundary layer in order to perform its mass transfer calculation for the reactions. The previous discretization used fifty – the maximum number of points possible – which means it requires the most computation time (Chen, 2011). Based on prior studies (Kucka et al., 2003) and looking at previous modeling work (Plaza, 2011), the number of discretization points was reduced without any loss of accuracy. The old and new discretizations are compared in Figure 12.

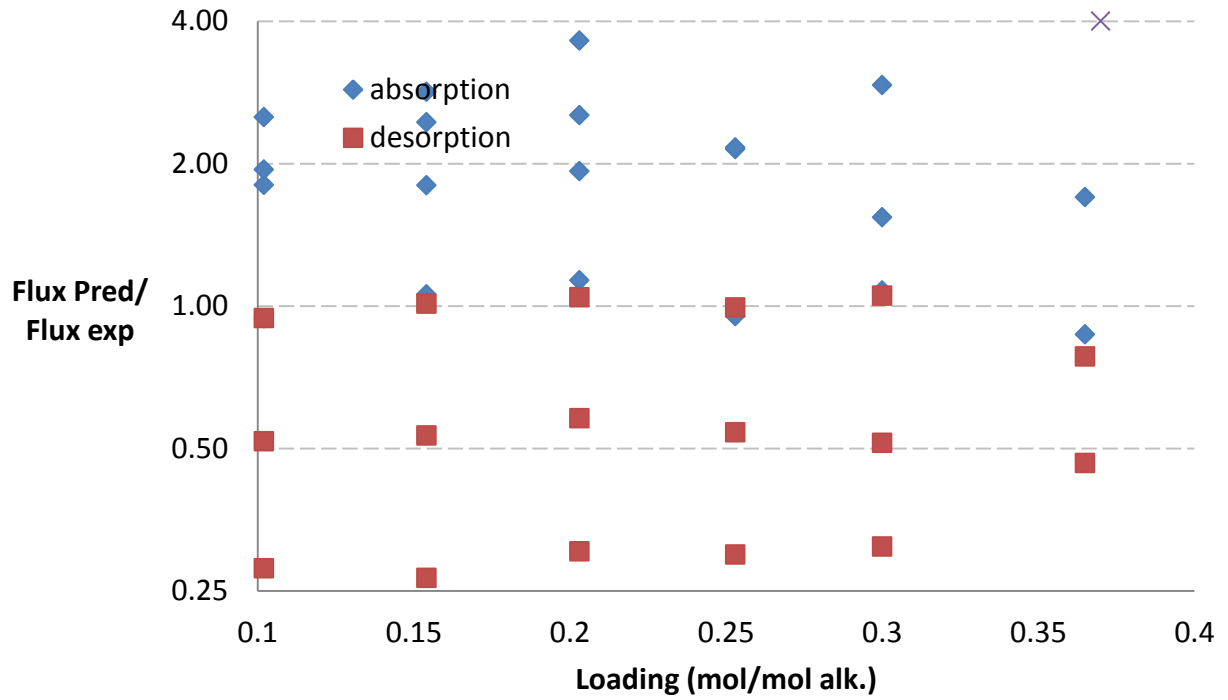


Figure 10: Model flux ratioed to experimental flux shows that the current kinetic model is overpredicting both absorption and desorption. Dashed lines delineate the operational loading range.

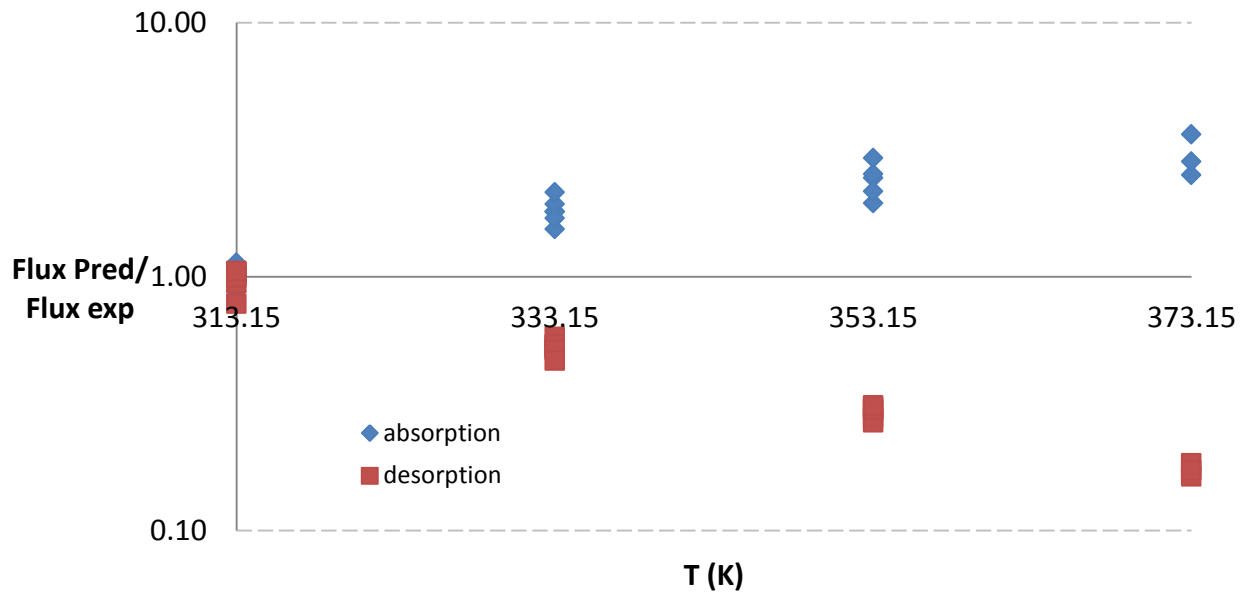


Figure 11: The fit of the kinetic data worsens at higher temperature in a symmetric fashion.

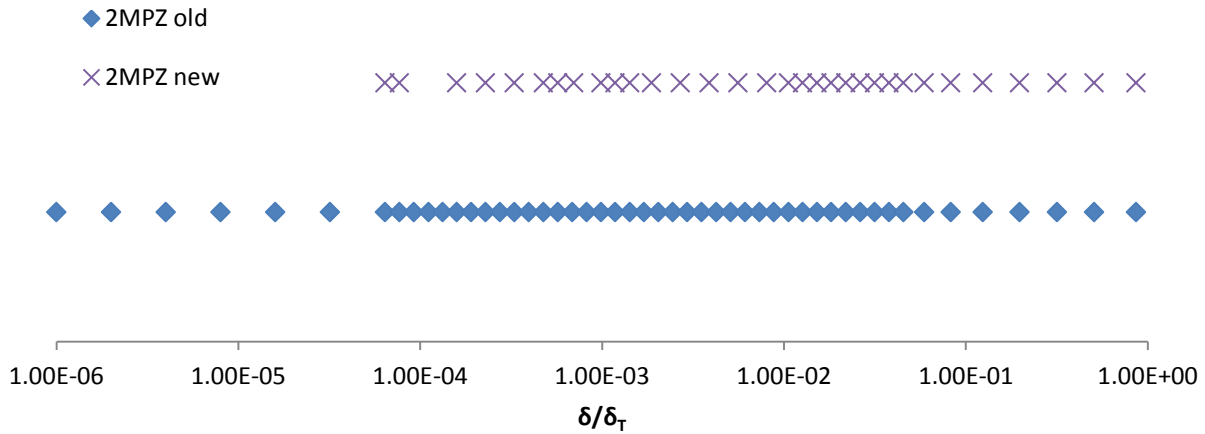


Figure 12: Boundary layer discretization. The x-axis is fraction through the boundary layer with the gas-liquid interface at left and the bulk liquid at right.

Conclusions

1. With increasing salt concentration, $P_{CO_2}^*$ decreased at lower loading and increased at higher loading.
2. By increasing alkalinity, the loading became richer while also showing the salt effect.
3. Both effects lead to reduced capacity, but have negligible effects on heat of absorption.
4. The boundary layer discretization was reduced, leading to faster computation time with no decrease in accuracy.

Future Work

Immediate objectives include finalizing the 8 m 2MPZ kinetic model to allow for process modeling and the construction of a heat exchanger model. Using 5 m 2MPZ viscosity data collected this quarter by Lynn Li, the process sensitivity to viscosity will be examined with particular interest in the sizing of the heat exchanger. A formal research proposal will be prepared in early May that will set the scope for all future work.

References

- Chen, X. *Carbon Dioxide Thermodynamics, Kinetics, and Mass Transfer in Aqueous Piperazine Derivatives and Other Amines*. The University of Texas at Austin. Ph. D. Dissertation. 2011.
- Cullinane, J. T. *Thermodynamics and Kinetics of Aqueous Piperazine with Potassium Carbonate for Carbon Dioxide Absorption*. The University of Texas at Austin. Ph. D. Dissertation. 2005.
- Frailie, P. T., Madan, T., Sherman, B. J., & Rochelle, G. T. (2013). "Energy performance of advanced stripper configurations." GHGT-11, Kyoto, Japan. 2012.

- Ko, J., & Li, M. “Kinetics of Absorption of Carbon Dioxide into Solutions of N-Methyldiethanolamine + Water.” *Chem Eng Sci.* 2008; 55:4139–4147.
- Kucka, L., Müller, I., Kenig, E. Y., & Górak, A. “On the Modelling and Simulation of Sour Gas Absorption by Aqueous Amine Solutions.” *Chem. Eng. Sci.* 2003; 58(16): 3571–3578.
- Plaza, J. M. *Modeling of Carbon Dioxide Absorption using Aqueous Monoethanolamine, Piperazine and Promoted Potassium Carbonate.* The University of Texas at Austin. Ph. D. Dissertation. 2011.
- Rochelle, GT et al. “CO₂ Capture by Aqueous Absorption, Third Quarterly Progress Report 2012.” Luminant Carbon Management Program. The University of Texas at Austin. 2012.